Original Article

Journal of Tissue Engineering
Volume 5: 1–13

DOI: 10.1177/2041731414551661
tej.sagepub.com
SAGE

Electrospun silk fibroin fiber diameter influences in vitro dermal fibroblast behavior and promotes healing of ex vivo wound models

Tom Hodgkinson[1,2], Xue-Feng Yuan[3] and Ardeshir Bayat[1]

Abstract

Replicating the nanostructured components of extracellular matrix is a target for dermal tissue engineering and regenerative medicine. Electrospinning *Bombyx mori* silk fibroin (BMSF) allows the production of nano- to microscale fibrous scaffolds. For BMSF electrospun scaffolds to be successful, understanding and optimizing the cellular response to material morphology is essential. Primary human dermal fibroblast response to nine variants of BMSF scaffolds composed of nano- to microscale fibers ranging from ~250 to ~1200 nm was assessed in vitro with regard to cell proliferation, viability, cellular morphology, and gene expression. BMSF support of epithelial migration was then assessed through utilization of a novel ex vivo human skin wound healing model. Scaffolds composed of the smallest diameter fibers, ~250 -300 nm, supported cell proliferation significantly more than fibers with diameters approximately 1 μm ($p < 0.001$). Cell morphology was observed to depart from a stellate morphology with numerous cell -fiber interactions to an elongated, fiber-aligned morphology with interaction predominately with single fibers. The expressions of extracellular matrix genes, collagen types I and III ($p < 0.001$), and proliferation markers, proliferating cell nuclear antigen ($p < 0.001$), increased with decreasing fiber diameter. The re-epithelialization of ex vivo wound models was significantly improved with the addition of BMSF electrospun scaffolds, with migratory keratinocytes incorporated into scaffolds. BMSF scaffolds with nanofibrous architectures enhanced proliferation in comparison to microfibrous scaffolds and provided an effective template for migratory keratinocytes during re-epithelialization. The results may aid in the development of effective BMSF electrospun scaffolds for wound healing applications.

Keywords

silk fibroin, electrospinning, biomaterials, nanofiber, primary human dermal fibroblasts

Received: 29 June 2014; accepted: 22 August 2014

Introduction

Bombyx mori silk fibroin (BMSF) materials and scaffolds for tissue engineering and regenerative medicine applications have been the subject of an increasing research interest.[1] The well-documented physical properties, benign chemical processing methods, and versatile end-point material formats of regenerated BMSF materials set them apart from other polymer systems. Several BMSF-based scaffolds have been developed with a porous architecture.[1–4] Greater emphasis is now being placed on the development of scaffolds with biomimetic architecture, with

[1]Plastic & Reconstructive Surgery Research, Manchester Institute of Biotechnology, University of Manchester, Manchester, UK
[2]School of Chemical Engineering and Analytical Science, University of Manchester, Manchester, UK
[3]National Supercomputer Centre in Guangzhou (NSCC-GZ), Research Institute for Application of High Performance Computing, Sun Yat-Sen University, Guangzhou, P.R. China

Corresponding author:
Ardeshir Bayat, Plastic & Reconstructive Surgery Research, Manchester Institute of Biotechnology, University of Manchester, 131 Princess Street, Manchester M1 7DN, UK.

several studies demonstrating the importance of the nanofibrous structure of the extracellular matrix (ECM) on cell function and tissue regeneration.[5–7]

Electrospinning can be used to fabricate uniform polymer fibers with diameters on the micro-/nanoscale.[8] Through adjustment of spinning solution composition, viscoelastic properties, and electrospinning process parameters, it is possible to control the morphology and diameter of electrospun fibers[8–13] (Supplementary Table 1). For BMSF, several solvent systems and electrospinning parameters have been employed for application in the engineering of various tissues.[11,13–23] Specifically for dermal engineering, a BMSF electrospun nanofiber matrix was shown to perform comparably to Matriderm, a commercially available skin substitute, in the treatment of a full-thickness murine skin defect.[24] Interestingly, the authors note that less contraction was evident in BMSF-treated wounds, which the authors attributed to the degradation rate of the fibroin matrix.[24] Aqueous BMSF solutions hold particular promise for the future inclusion of instructive cues due to elimination of harsh chemical reagents and fabrication conditions. Due to their intrinsic viscoelastic properties, aqueous BMSF solutions are commonly blended with high-molecular weight (Mw) polymers, such as poly(ethylene oxide) (PEO), which act as rheological modifiers and significantly enlarge the electrospinning processing window.[13,25]

The potential of these BMSF electrospun scaffolds to support the attachment and proliferation of human cells is well documented.[8,11,12,16,26] Cell morphology and focal adhesion formation/spatial organization effect cell signaling.[27] Through this, fiber morphology and arrangement have the potential to considerably alter cell activity and in turn, a biomaterial's efficacy.[28] Several investigators have examined the link between electrospun fiber diameter and cell behavior, with as of yet no clear consensus. Chen et al.[29] showed proliferation of NIH 3T3 fibroblasts was highest on polycaprolactone scaffolds with fibers of 428 nm (the smallest uniform fibers they obtained) and decreased as fiber diameter increased. Kumbar et al.[30] reported increased adherence, spreading, and proliferation of dermal fibroblasts on polylactide-*co*-glycolide (PLGA) fibers with diameters of 250–467, 500–900, and 600–1200 nm compared to 150–225, 200–300, 2500–3000, and 3250–6000 nm. Neural stem cells cultured on polyethersulfone substrates of ~283 nm showed increased proliferation and spreading compared to cells cultured on ~749 and ~1452 nm fibers.[31] Several authors have also reported increases in cell proliferation in micron sized in comparison to submicron fibers.[32,33] Osteo-progenitor cells proliferated more rapidly with increasing poly(lactic acid) and poly(ethylene glycol)–poly(lactic acid) fiber diameter.[33]

Currently, to the best of our knowledge, only one comparative study on cell growth between nanofibrous and microfibrous electrospun BMSF scaffolds exists in the literature and uses human umbilical vein endothelial cells (HUVECs).[34] In this study, Bondar et al. report that cell proliferation was comparable between nano- and microfibrous scaffolds, though cell attachment and in vivo–like cell morphology were promoted on nanofibrous scaffolds.

The varying nature of these reports and absence of a systematic study for BMSF electrospun materials means that there is a pressing need for the assessment of the effect of fiber diameter on human-derived cells such as dermal fibroblasts. In vitro systems provide valuable cell-material response information, but lack the complexity and architecture of natural cutaneous tissue. In order to pre-clinically assess the performance of BMSF electrospun scaffolds, we developed and implemented an ex vivo, full-thickness, human skin wound healing model. This model is similar to other published cutaneous wound healing models[35] and is designed to allow the comparison of epidermal migration in response to artificial wounding.

Materials and methods

Preparation of regenerated BMSF-PEO aqueous solutions and electrospinning

Concentrated aqueous BMSF solutions were generated as previously described[13] (see Supplementary Methods). BMSF concentration was determined by dry weight analysis of solutions. Solution pH was measured as pH 8–8.5 without adjustment and surface tension for all tested solutions was 0.05 N m^{-1} at 20°C.

To closely control fiber diameter in the fabricated scaffolds, pure BMSF aqueous solutions were blended with PEO (Dow Chemicals Ltd, USA). This was determined by Li et al.[36] to have a molecular weight of $M_w = 4.82 \times 10^6$ g/mol by gel permeation chromatography. The overlap concentration, c*, was calculated (see Supplementary Methods) to be 0.0206 wt%. BMSF-PEO solutions were created containing PEO to a concentration of 0.206 wt%, which equates to 10c* concentration. This was selected as an excellent spinning dope from our previous, detailed research examining the effects of BMSF and PEO concentration, along with differing electrospinning conditions, on solution rheology and fiber formation.[13]

BMSF-PEO solutions were electrospun using in-house electrospinning apparatus. Solutions of 10 wt% BMSF/10c* PEO were loaded into a 10-mL syringe (BD Bioscience, UK) and pushed through a connecting tube and blunt-tipped stainless steel needle (inner diameter 0.5 mm). The solution was pumped at various speeds and a range of voltages applied. The high-voltage power supply used in this study was able to apply a maximum of 30 kV.[13]

Characterization of nanofibrous scaffolds

To produce fibers with varying diameters, the BMSF-PEO solutions were spun under various electrospinning process parameter conditions. The resultant fibers were analyzed, after insolubilization treatment by submersion in 100% (v/v) methanol for 10 min at room temperature, through scanning electron microscopy (SEM) of gold sputter-coated samples (FEI Quanta 200 (E) SEM + energy-dispersive X-ray (EDX); FEI, USA). Fibers to be used in this study were selected on the basis of their fiber diameter and standard deviations. Fiber measurements were conducted using ImageJ Software v1.45 (NIH, USA). To calculate diameter, 50 fiber diameters were measured at random to obtain mean diameter and standard deviation. For histograms of fiber diameter distribution, numbers of fiber diameters were converted into percentage total values and plotted against grouped fiber diameter. The mean fiber diameters are shown, along with standard deviations (Figure 1; Table 1).

Primary human dermal fibroblast extraction, seeding, and assessment of proliferation and viability

Primary human dermal fibroblasts (PHDFs) were obtained from five Caucasian male and female patients undergoing elective surgery with full written consent and ethical approval. Viable cells were extracted from tissue according to protocols previously established in our laboratory.[37] Briefly, tissue samples were minced and cells were released through enzymatic digestion with Collagenase A (Roche Diagnostics, UK) overnight at 4°C. Subsequently, digested tissue was mixed by pipette and cultured in cell-bind culture flasks and incubated at 37°C/5% (v/v) CO_2. Fibroblasts were expanded in culture and cells below passage 5 utilized.

PHDFs were seeded at 1×10^4 cells per well of 96-well culture plate. The effects of electrospun fiber diameter on PHDF proliferation were compared through the MTT assay (Roche Diagnostics), performed according to the manufacturer's instructions (see Supplementary Methods). The optical density (OD) of 100 µL of the reaction mix was measured at wavelength OD 550 nm (corrected for OD 690 nm).

The lactate dehydrogenase (LDH) assay (Roche Diagnostics) was used to assess the effect of fiber morphology on PHDF viability, performed according to the manufacturer's instructions (see Supplementary Methods). Absorbance was measured at OD 492 nm (corrected for OD 690 nm). For MTT and LDH assays, the results represent means of three independent assay reactions, for five different PHDF populations.

RNA extraction, complementary DNA synthesis, and gene expression analysis through quantitative real-time polymerase chain reaction

RNA was extracted using the RNeasy Kit (Qiagen, UK) according to the manufacturer's instructions. RNA concentration was determined using a NanoDrop ND-1000 (Labtech International, UK) and normalized for complementary DNA (cDNA) synthesis reaction (qScript™ cDNA SuperMix (Quanta Biosciences, USA)). Quantitative real-time polymerase chain reactions (qRT-PCRs) were performed using the Lightcycler 480 II platform (Roche Diagnostics). Gene expression levels were further normalized with an internal reference gene, ribosomal protein L32 (RPL32). For a list of primer sequences used in this study, please refer to Supplementary Table 2.

Immunocytochemical staining

To analyze the effect of fiber diameter on PHDF morphology, immunocytochemical staining for α-tubulin was used. Cells were fixed, permeabilized, blocked, and incubated in primary antibodies for α-tubulin (Abcam, UK; ab80779, 1:250) 1 h at room temperature. After washing, secondary antibodies (Alexa Fluor 488) (1:500) were added (1 h/room temperature). Nuclei were stained with 4′,6-diamidino-2-phenylindole (DAPI) (1:500) (Life Technologies, UK). Cell morphologies were imaged using an Olympus BX51 (Olympus, UK).

Ex vivo wound healing model

Full-thickness skin was obtained from three Caucasian male and female patients undergoing elective surgery with full written consent and ethical approval. Skin was washed in phosphate buffered saline (PBS), a 4-mm biopsy taken, and surrounding this, a larger 8-mm biopsy taken, leaving a doughnut shape. These were inserted into 24-well inserts (pore size 3.0 µm; Corning, USA). To fill the wounded portion of the tissue, 5-mm disks were cut from electrospun BMSF scaffolds (fiber diameter 256 nm ± 30 nm). These were carefully inserted into the wounded portion and complete Dulbecco's Modified Eagle Medium (DMEM) was added to the outside of the well so that the epidermis was at the liquid–air interface (Figure 2). The epidermal keratinocytes at the wound boundaries were then allowed to migrate in response to injury across the wound area, with and without BMSF scaffold incorporation. The migration was then investigated through hematoxylin and eosin (H&E) staining of wound cross sections after 1 and 2 weeks of culture. The migration of cells was quantified through measurement of the length of migratory epidermal tongue structures

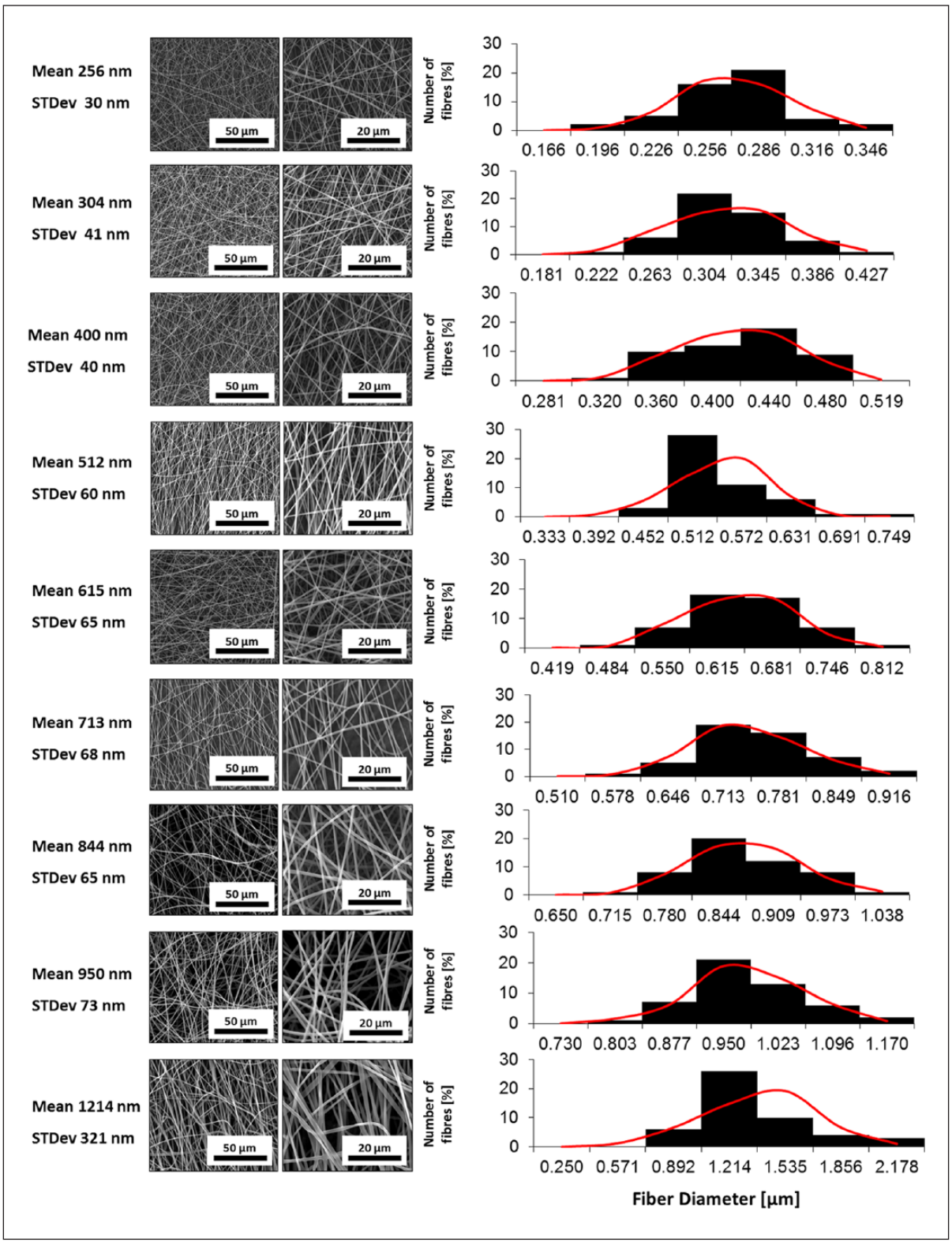

Figure 1. Representative scanning electron micrographs of BMSF scaffolds and fiber diameter distribution histograms. Red curves indicate normal distributions calculated using the means and standard deviations of each fiber set.
BMSF: *Bombyx mori* silk fibroin.

Table 1. Electrospinning parameters and resulting BMSF fiber diameters.

Electric field (kV/cm)	Spinneret height (cm)	Flow rate (mL/h)	Mean fiber diameter (nm)
0.95	30	1	256 ± 30
0.8	30	0.5	304 ± 41
0.85	20	0.5	400 ± 49
0.5	25	0.75	512 ± 60
0.65	20	0.75	615 ± 65
0.5	20	0.75	713 ± 68
0.6	30	0.75	844 ± 65
0.55	30	0.75	950 ± 73
0.5	30	0.75	1214 ± 321

BMSF: *Bombyx mori* silk fibroin.

into the wound for each patient, and a mean distance was taken and expressed as a percentage of total wound width. The medium was changed daily throughout the culture period.

Statistical analysis

The comparison of cell proliferation, viability, and gene expression between BMSF scaffold fibers of varying diameters was statistically tested using independent T-tests of five independent triplicates using five different cell populations. Independent T-tests were also used to assess the migration of keratinocytes from wound edges in ex vivo wound models using data from three patients. All data were analyzed using IBM SPSS Statistics Software version 19.0 (SPSS Inc., Chicago, IL, USA). Significant values were considered as those where $p < 0.05$.

Results

Decreasing fiber diameter increases PHDF proliferation and viability in vitro

Through control of electrospinning solution properties and process parameters,[13] scaffolds of uniform BMSF fibers were generated and scaffolds of increasing fiber diameter were chosen for analysis from 256 ± 30 to 1214 ± 321 nm (Figure 1). To assess the effects of electrospun BMSF fiber diameter on cell proliferation in culture, MTT assays were performed to quantify viable cell number up to 14 days (Figure 3). Initial proliferation in the first 48 h of culture was comparable between scaffolds. After 72 h, PHDF proliferation on BMSF scaffolds with fibers ~250–300 nm in diameter was increased in comparison with larger diameter fibers. After 1 week, there is a highly significant difference in cell proliferation between fibers below 304 nm in diameter and those 400 nm and above, with a general trend of decreasing proliferation for increasing fiber diameter. Interestingly, the largest increase in cell number is observed between cells cultured on scaffolds ~300 and ~400 nm. The proliferation in scaffolds between ~850 and ~1200 nm was comparable during culture. Optimal cell proliferation was seen in scaffolds with the smallest fiber diameters, approximately 250–300 nm ($p < 0.001$) (Figure 3).

Cell viability was comparable across all BMSF scaffolds, though up to 72 h and 1 week culture those scaffolds composed of nanofibers below 400 nm in diameter showed higher cell viability (Figure 4). When the results of the LDH assays are taken together with MTT results, viable cell numbers are significantly improved in nanofibrous BMSF electrospun scaffolds.

Fiber diameter affects PHDF morphology

The morphology of cells on electrospun scaffolds of increasing fiber diameter was compared using fluorescent microscopy. Cells were stained for nuclei and α-tubulin (Figure 5) up to 7 days. After 24 h, cell morphology across all fiber diameters was similar and rounded, which is characteristic of poorly attached cells. As BMSF does not possess any integrin binding motifs, this is perhaps unsurprising. After 72 h, cells cultured on fibers ~250 and ~500 nm showed attachment to multiple fibers and a spread morphology. As fiber size increased up to ~1200 nm, cells were increasingly seen to align themselves to single fibers, taking on elongated morphologies. After 7 days, cells adopted a mature, scaffold-dependent phenotype. Cells cultured on fibers with diameters >1 μm showed an elongated morphology, with filopodal projections up to hundreds of microns in length, anchoring the cell physically to the scaffold (Figure 5). Intermediate cell morphologies were seen in fibers ~500 and ~850 nm, with fewer cells adopting elongated morphologies. In scaffolds with fiber diameters ~250 nm, cells were spread between multiple fibers and stellate in appearance.

Fiber diameter affects gene expression of PHDFs

In general, the expression of collagen types I and III was increased in PHDFs cultured on BMSF scaffolds with nanofibers ~250 nm in comparison to larger fibers ($p < 0.0001$) (Figure 6). Interestingly, the expression of both collagens I and III by 7 days of culture was influenced on the diameter of BMSF fibers in scaffolds with a stepwise decrease in fibers ~500–700 nm and ~850–1200 nm. When the ratio of the relative expression of types I–III collagen is examined, there is a difference between cells cultured on the different fibers. After 3 days of culture, the greatest ratio of collagen III to collagen I was observed on the largest diameter fibers (1214 ± 321 nm). The lowest expression of collagen III relative to collagen I was observed in intermediate

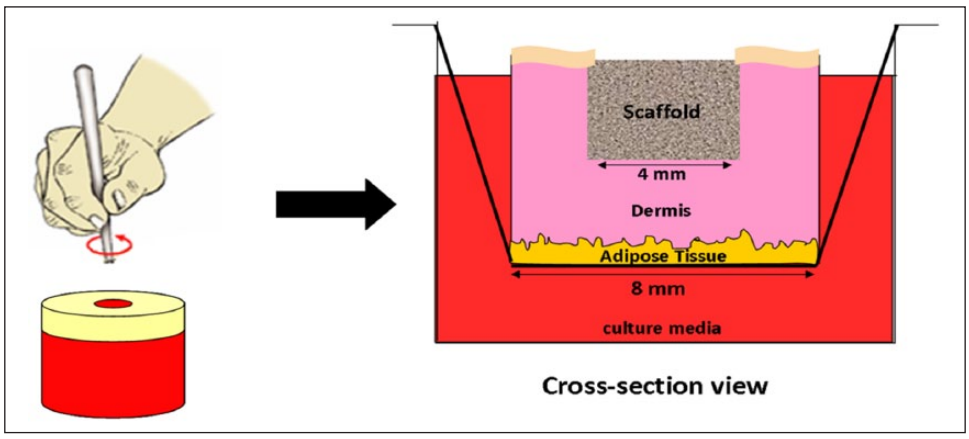

Figure 2. Diagram showing ex vivo wound healing assay experimental design. Full-thickness skin is cut into 8-mm biopsies and wounded with a further 4-mm punch. The skin is inserted into a well insert and the wound filled with the BMSF scaffold. Medium was added to the well, leaving the epidermis air exposed.
BMSF: *Bombyx mori* silk fibroin.

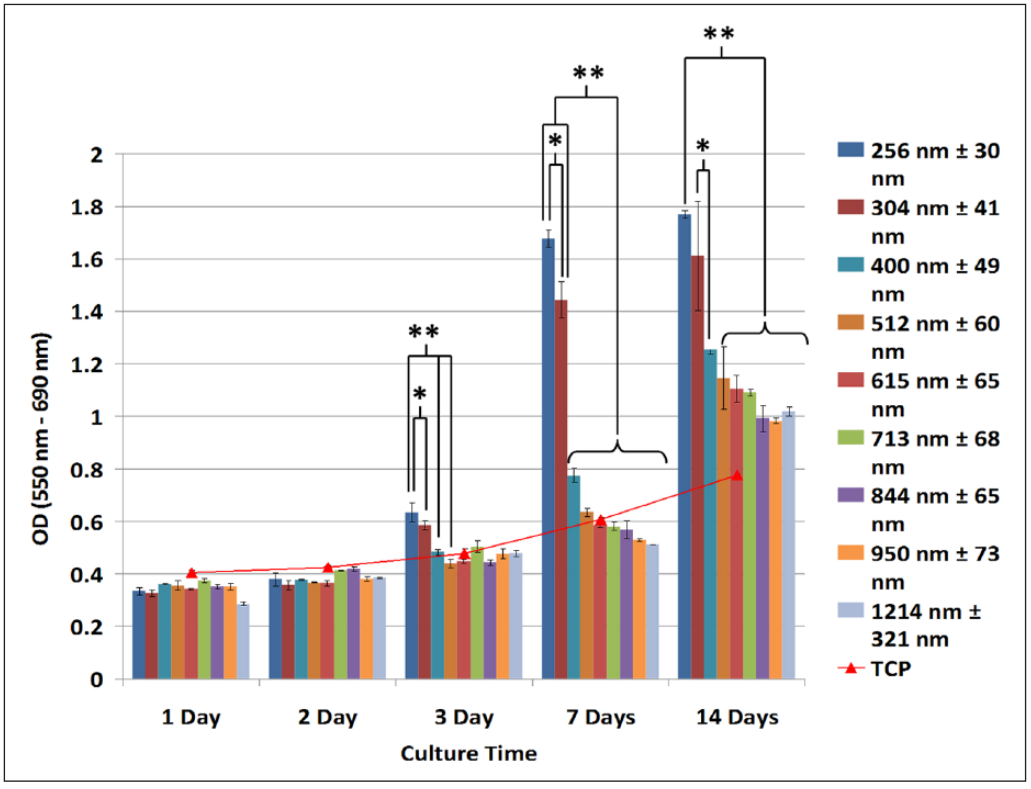

Figure 3. MTT analysis of cell proliferation on BMSF fibrous scaffolds. Cell proliferation in 256 and 304 nm diameter fibrous scaffolds is significantly enhanced during the culture period (*$p < 0.05$; **$p < 0.001$). Values are means of five independent experiments performed in triplicate with five different PHDF populations.
BMSF: *Bombyx mori* silk fibroin; PHDF: primary human dermal fibroblast; OD: optical density.

PHDF interaction with BMSF scaffolds in a systematic manner in an effort to optimize scaffold design for skin regeneration applications.

The diameter of fibers was found to directly influence cell attachment and morphology, proliferation, viability, and gene expression within scaffolds. Ongoing cell proliferation in culture was best supported by fibers ~250–300 nm in diameter, with cell proliferation decreasing as fiber size increased until diameters of approximately 850 nm, above which cells showed similar proliferation

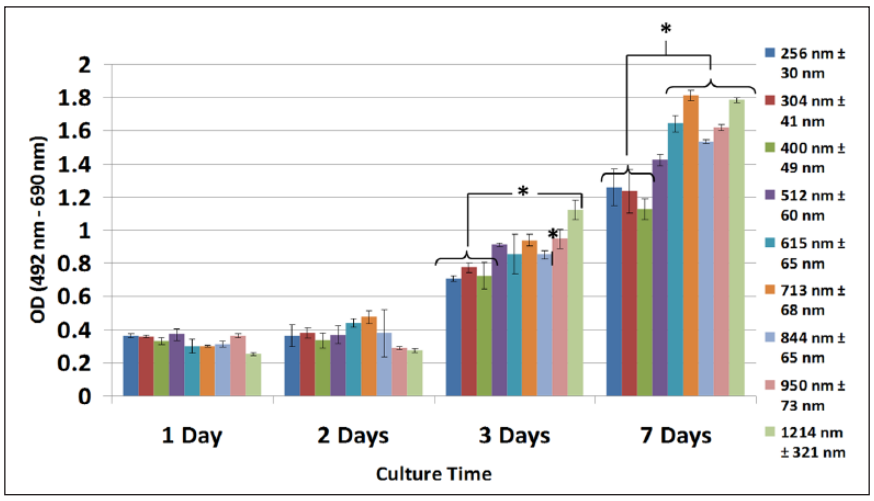

Figure 4. LDH analysis of cell viability in BMSF fibrous scaffolds. Cell viability between scaffolds is comparable, with increased viability observed after 7 Days in nanofibrous scaffolds with fiber diameters <400 nm, as seen by lower absorbance (*$p < 0.05$). Values are means of five independent experiments performed in triplicate with five different PHDF populations.
LDH: lactate dehydrogenase; BMSF: *Bombyx mori* silk fibroin; PHDF: primary human dermal fibroblast; OD: optical density.

fibers (713 ± 68 nm). Fibers of ~250, ~512, and ~844 nm have collagen I to collagen III expression ratios of approximately 3:1. After 7 days, the relative expression of collagen III in cells cultured on fibers ~1214 nm decreases, approaching expression ratios in cells on other fibers of approximately 1:0.3 (collagen I:collagen III). When the expression of collagens I and III is compared between 3 and 7 days of culture, a decrease in relative gene expression is observed. Such a relative decrease could indicate a cell-synthesized collagen-saturated environment after 7 days in culture, resulting in decreased collagen expression stimulus.

The expression of proliferating cell nuclear antigen (PCNA) was highest in cells cultured on fibers 512 nm in diameter and below (3 and 7 days; $p < 0.0001$). The elevated expression of PCNA in cells cultured on smaller fiber diameters corresponds to MTT data showing increased cell proliferation. Expression of focal adhesion kinase (FAK) was comparable for BMSF fibers of different diameters. At 3 days of culture, there was a significant increase in FAK expression in comparison to micron-sized fibers, though this effect was not carried forward to 7 days of culture. This relative decrease in expression could be as a result of high cell density and an overall decrease in cell migration and in turn dynamic focal adhesion formations. These data suggest that similar amounts of focal adhesions are in place for cells, independent of fiber diameter.

Electrospun BMSF scaffolds promote re-epithelialization in an ex vivo wound healing model

To investigate the ability of BMSF scaffolds to support re-epithelialization, an ex vivo cutaneous wound model was developed and employed. BMSF electrospun scaffolds facilitated the migration of epithelial cells from the wound margin of ex vivo models in comparison to unassisted wounds (Figure 7). The epithelial tongue was seen to migrate along the base of the BMSF scaffold over 2 weeks of culture, where the scaffold and the underlying existing collagenous matrix of the dermis meet. Cell position within the BMSF matrix indicates that the cells employ it as a guide for migratory tongues with morphology comparable to those seen in vivo. Quantification of epithelial tongue migration showed that in ex vivo models where BMSF scaffolds were applied, keratinocyte migration was significantly increased at both 7 and 14 days ($p = 0.019$ and $p = 0.0034$, respectively) (Figure 7(c)). In those models where BMSF was applied, 92% of the wound width was closed by epithelial migration in comparison to 20.5% in wounds without scaffolds. Though degradation of scaffolds was not quantified during the study, scaffolds remained intact after the culture period and no notable fiber degradation was observed through microscopic examination. The degradation of the scaffolds is likely to be dramatically different in an in vivo wound environment, but in other studies has been shown to be tunable through alteration of BMSF secondary protein structure.[38,39]

Discussion

In the development of successful BMSF scaffolds, it is crucial to optimize physical architecture and properties for cell growth and scaffold population in the wound. At present, the effects of scaffold physical properties such as fiber morphology on cell attachment, spreading, proliferation, and gene expression are not well studied in BMSF scaffolds. This study directly links fiber morphology with

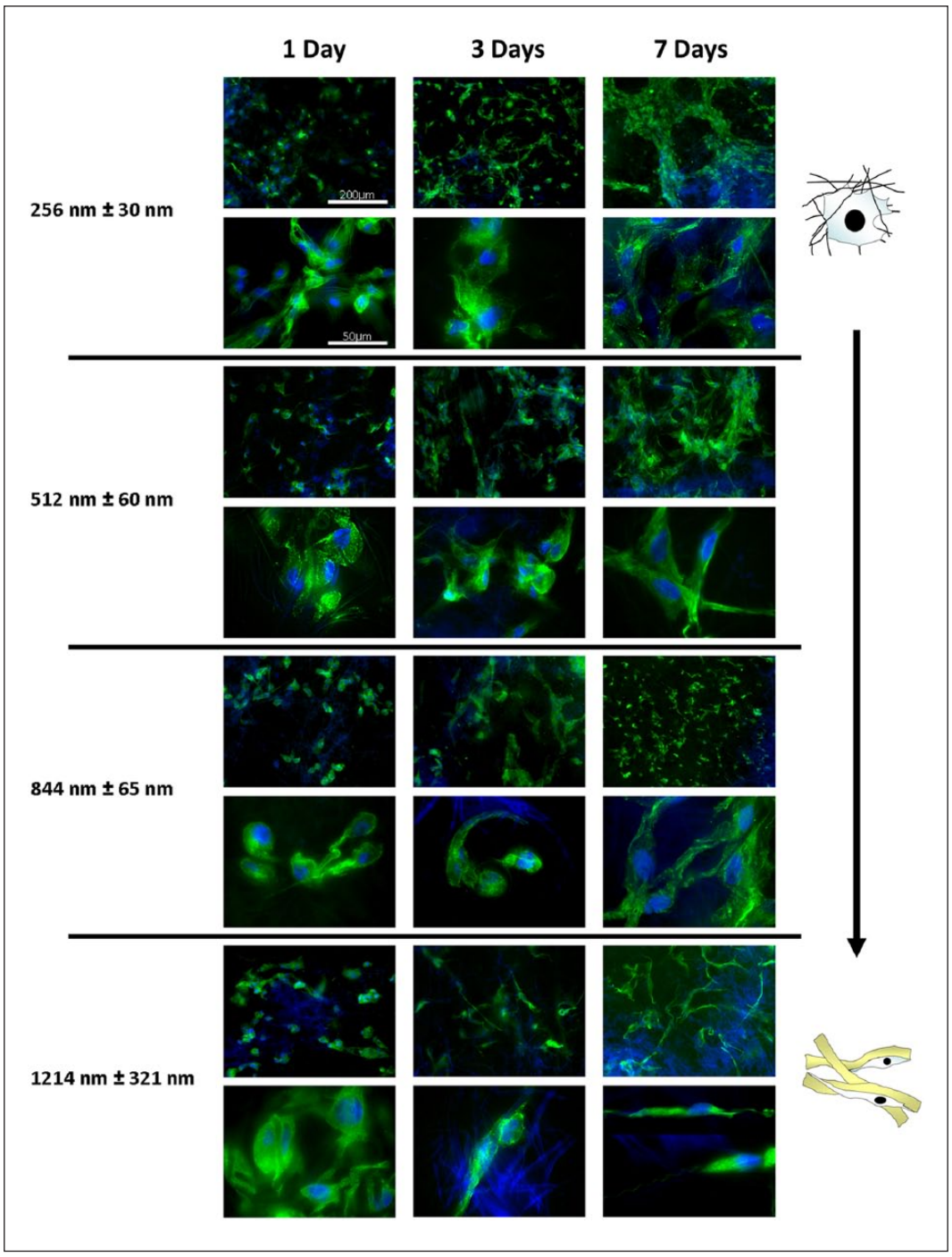

Figure 5. Effect of fiber diameter on PHDF morphology. Representative immunofluorescence (alpha tubulin (green); DAPI (blue)) images of PHDF morphology cultured on different scaffolds at 7 Days. As fiber diameter increases, the morphology of cells becomes more elongated and cells are seen to progressively adhere to single fibers, forming long filopodal extensions. On nanofibers, cells form multiple attachment sites between fibers and take a spread, stellate morphology.
PHDF: primary human dermal fibroblast; DAPI: 4′,6-diamidino-2-phenylindole.

characteristics as on micron-sized fibers. The results obtained here agree, in part, with previous reports using other polymer systems for fiber formation.[30,31,40] However, other reports exist demonstrating greater cell proliferation in cells cultured on micron-sized fibers.[33,34] Though no previous study using BMSF electrospun fibers has examined as many fiber diameters as reported here, the results obtained taken together with a previous work indicate fibers in the range of ~250 nm promote cell proliferation. Having said this, a nanoscale scaffold is not required for cells to proliferate well and larger fibers, which may be perceived by cells as two-dimensional

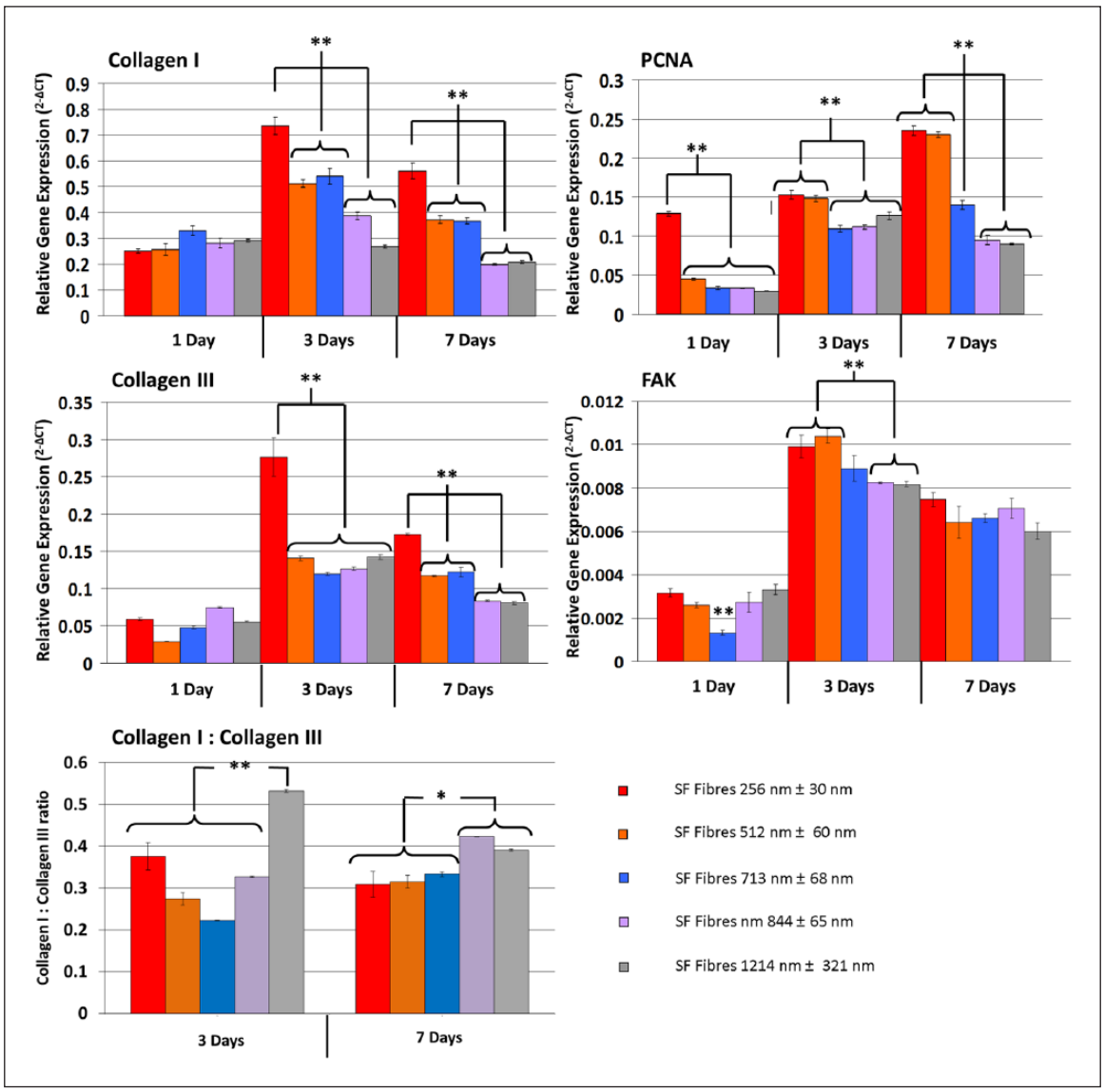

Figure 6. Comparison of gene expression of PHDFs cultured on BMSF scaffolds of varying fiber diameter. The differences in relative gene expression between PHDFs cultured on increasing fiber diameter show a decrease in collagen I and collagen III expression with increasing fiber size. PCNA expression increased in nanofibrous scaffolds (**$p < 0.001$). There were significant differences between smaller diameter fibers and larger fibers at day 3 but comparable levels of FAK after 7 Days of culture (**$p < 0.001$). Values are means of three independent experiments performed in triplicate with three different PHDF populations. PHDF: primary human dermal fibroblast; BMSF: *Bombyx mori* silk fibroin; PCNA: proliferating cell nuclear antigen.

surfaces, may also allow rapid cell proliferation. Scaffolds composed of fibers of this morphology may result in cells adopting an artificial morphology, which in turn may affect the expression of cell adhesion and tension-sensitive expression pathways. These may be of particular importance in the prevention of pathological scarring or contracture in cutaneous wound healing.[40,41] It is logical therefore to aim for a biomimetic architecture in artificial scaffolds.

The collagenous fibers of the dermal ECM range from 30 to 50 nm for individual fibrils to 500 nm for fully assembled fibrous structures (type I collagen fibrils 50 nm; type III collagen fibrils 30–130 nm) and are therefore on a similar size scale to the most successful of the BMSF test scaffolds.[42] One possibility is that the response of cells to the smallest nanofibers produced here could be a reflection of their similarity in size to immature collagen fibrils seen during wound healing. In this scenario, the size of these fibers could themselves promote a wound healing phenotypic response (cell proliferation, ECM production, increased migration, etc.). As with proliferation studies, previous literature examining the effect of BMSF electrospun fiber diameter on cell attachment and spreading is sparse and evidence must be pooled from different cell types, BMSF solvent systems, scaffold processing methods, and from isolated studies where one or two fiber

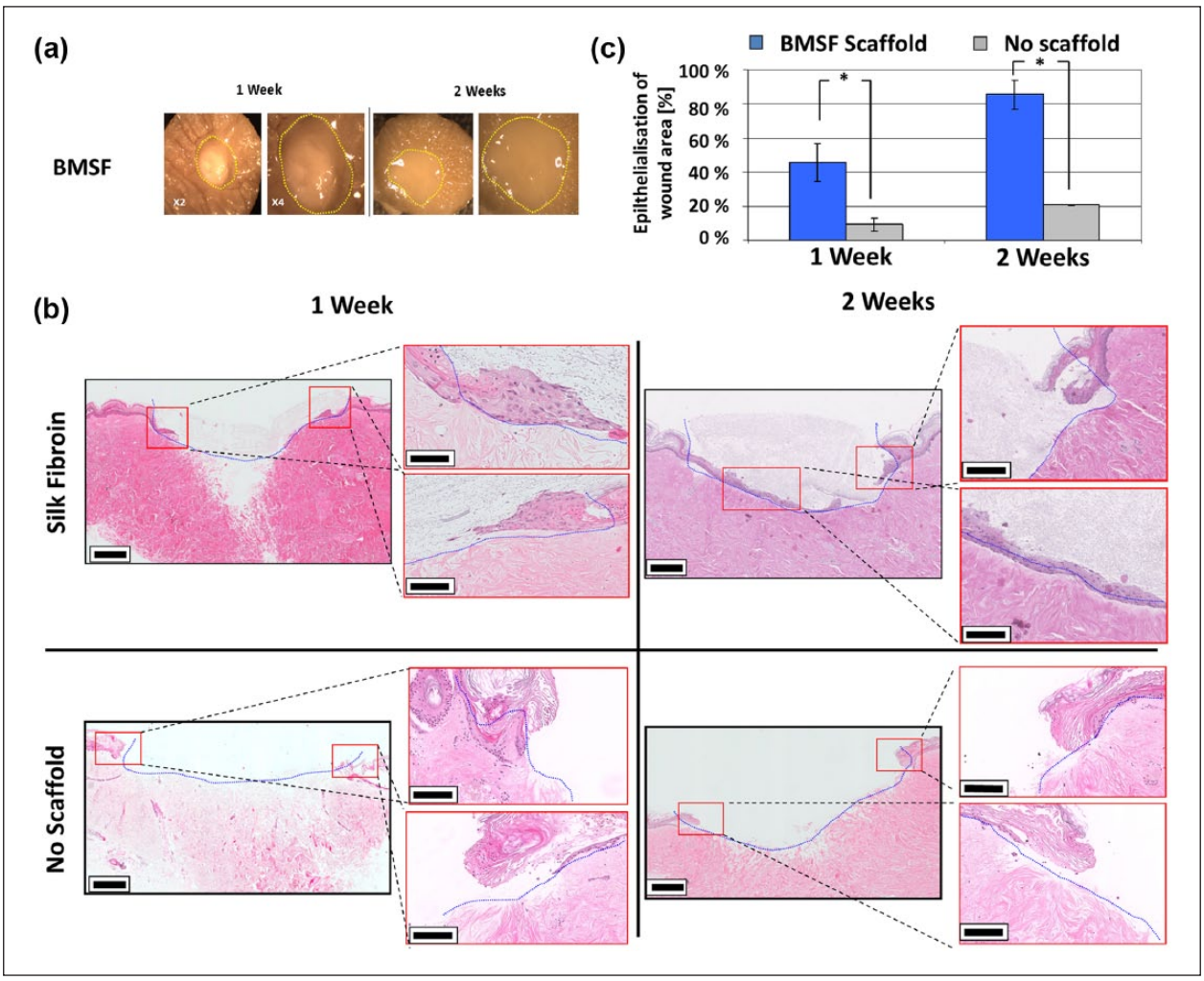

Figure 7. BMSF electrospun scaffolds promote re-epithelialization of ex vivo wound model. (a) Stereomicroscopic images of ex vivo wound healing models treated with BMSF electrospun scaffolds after 1 and 2 weeks. Yellow lines show the original wound boundary. Stereomicroscopic images show little discernable difference during culture. (b) Representative hematoxylin and eosin–stained wound cross sections of BMSF-assisted and -unassisted artificial wounds. Re-epithelialization is significantly more advanced at both 1 and 2 weeks in BMSF scaffold–filled wounds. Blue lines represent the original wound boundary. Red boxes show wound boundaries, which are magnified for clarity. (c) Comparison of migration of epithelial tongue after 1 and 2 weeks of ex vivo culture in wounds treated with BMSF scaffolds and those without scaffold assistance (*$p < 0.05$).
BMSF: *Bombyx mori* silk fibroin.

diameters are examined. This situation does not allow the accurate comparison between studies of the effect of fiber diameter in BMSF scaffolds. The ability to fabricate uniform fibers over a range of diameters in this study meant that the results presented offer a more detailed picture of the relationship between fiber diameter and PHDF behavior while avoiding overlap in fiber diameter between groups. Although previous work has investigated the effect of fiber size on a cellular level, it should be emphasized that the findings between different polymer systems and cell sources may not be comparable. Differing polymers possess different intrinsic physiochemical properties that in turn affect protein adsorption to the scaffolds, affecting cell spreading and proliferation. While cell sources may be differentially affected by integrin-mediated cell signaling or other external physical environments and morphologically related signals.

Immunofluorescent labeling showed that cells adopt differing morphologies and adherence strategies dependent on fiber diameter, with fibers ~250 nm resulting in multiple cell adhesions over multiple fibers. As fiber size increased, cell attachment was seen to become more dependent on single-fiber adhesions, effectively rendering the surface as a two-dimensional plane for cell adhesion. Cells became elongated along fiber lengths, a feature that may be useful to exploit for other applications where this morphology may be advantageous, such as nerve tissue engineering.[43,44] Previous work comparing scaffolds

composed of nano- and microfibrous scaffolds reported similar morphological changes and increases in cell attachment.[34,40] From gene expression analysis, it is clear that this attachment morphology corresponds with expression of proliferation genes and ECM production. This result is in agreement with studies in other polymer systems.[45,46] The increased expression of FAK in the smallest diameter fiber scaffolds may suggest more dynamic focal adhesion formation, which may facilitate cell migration into the scaffold, allowing in turn greater cell proliferation. When type I collagen to type III collagen expression is compared in the scaffolds, there is an increase in the ratio of collagen III to collagen I in the largest fiber diameter scaffolds, though the lowest collagen expression overall. Other fiber diameters have collagen I to III ratios of approximately 3:1, similar to what others have reported for normal skin fibroblasts in culture.[47,48] Increased collagen III expression is associated with younger skin and reduced scarring,[37] though examination under in vivo conditions would be required to validate the change in collagen I to collagen III ratio observed here. Furthermore, the changes in expression ratios are small and transient in nature, reducing to a similar range to all scaffolds after 7 days of culture.

The developed ex vivo model provides a structurally comparable model to natural skin and allows a pre-clinical assessment of the ability of BMSF scaffolds to support re-epithelialization. Use of the BMSF scaffolds increases re-epithelialization in this model over unassisted wounds to a high-level statistical significance at both 7 and 14 days ($p = 0.019$ and $p = 0.0034$, respectively). Although the migration of cells within this model is slower than the natural setting, due to a reduction of wound healing cytokine and chemokine signaling and a lack of blood flow, it provides a quantifiable comparison of scaffold effectiveness. The preservation of surrounding tissue architecture and cellular complexity mean that alongside in vitro assays, the ex vivo model is suitable for the assessment of cellular interaction with the scaffold during the events of re-epithelialization. Though in vivo animal models are still essential, utilization of this model could help to reduce the number of animal experiments required.

Previous work in vivo comparing BMSF electrospun scaffolds to matrigel in mice showed very similar healing rates but an improved healing outcome when using BMSF, with less contraction and complete degradation of the transplanted scaffold during tissue remodelling.[24] This work optimizing the architecture of BMSF scaffolds is likely to improve their wound healing ability further and through the validated ex vivo model presented here it will be possible to compare their performance prior to in vivo testing. The utility of BMSF scaffolds as dermal substitutes is likely to not be confined to cutaneous wound healing and due to the ease of architectural modification during the electrospinning process could be optimized for further applications. At present, other dermal substitutes, such as decellularized dermis, are finding application in breast implant surgery in efforts to reduce contracture.[48–51]

Conclusion

In conclusion, the diameter of electrospun fibers was shown to directly influence the proliferation, morphology, and gene expression of PHDFs. Fiber diameters ~250–300 nm were found to support significantly more cell proliferation and cell spreading, which decreased as fiber diameter increased. Cells expressed ECM, cell proliferation, and attachment genes to a greater extent on these small fiber diameter scaffolds. Ex vivo wound healing models demonstrated that BMSF scaffolds support keratinocyte migration and promote wound closure in comparison to unassisted wounds.

Acknowledgements

The authors wish to acknowledge Dr Paddy Hill at the School of Chemical Engineering and Analytical Science, University of Manchester, for assistance in scanning electron microscopy.

Declaration of conflicting interests

The authors declare no conflict of interest.

Funding

This research received no specific grant from any funding agency in the public, commercial, or not-for-profit sectors.

References

1. Rockwood DN, Preda RC, Yücel T, et al. Materials fabrication from *Bombyx mori* silk fibroin. *Nat Protoc* 2011; 6(10): 1612–1631.
2. Altman GH, Diaz F, Jakuba C, et al. Silk-based biomaterials. *Biomaterials* 2003; 24(3): 401–416.
3. Pritchard EM and Kaplan DL. Silk fibroin biomaterials for controlled release drug delivery. *Expert Opin Drug Deliv* 2011; 8(6): 797–811.
4. Kundu B, Kurland NE, Bano S, et al. Silk proteins for biomedical applications: bioengineering perspectives. *Prog Polym Sci* 2014; 39(2): 251–267.
5. Gertz CC, Leach MK, Birrell LK, et al. Accelerated neuritogenesis and maturation of primary spinal motor neurons in response to nanofibers. *Develop Neurobiol* 2010; 70(8): 589–603.
6. Erisken C, Zhang X, Moffat KL, et al. Scaffold fiber diameter regulates human tendon fibroblast growth and differentiation. *Tissue Eng Part A* 2012; 19(3–4): 519–528.
7. Chandrasekaran AR, Venugopal J, Sundarrajan S, et al. Fabrication of a nanofibrous scaffold with improved bioactivity for culture of human dermal fibroblasts for skin regeneration. *Biomed Mater* 2011; 6(1): 015001.
8. Min B-M, Lee G, Kim SH, et al. Electrospinning of silk fibroin nanofibers and its effect on the adhesion and spreading of normal human keratinocytes and fibroblasts in vitro. *Biomaterials* 2004; 25(7): 1289–1297.

9. Sill TJ and Von Recum HA. Electrospinning: applications in drug delivery and tissue engineering. *Biomaterials* 2008; 29(13): 1989–2006.
10. Zhang F, Zuo B, Fan Z, et al. Mechanisms and control of silk-based electrospinning. *Biomacromolecules* 2012; 13(3): 798–804.
11. Jin H-J, Chen J, Karageorgiou V, et al. Human bone marrow stromal cell responses on electrospun silk fibroin mats. *Biomaterials* 2004; 25(6): 1039–1047.
12. Zhang X, Baughman CB and Kaplan DL. In vitro evaluation of electrospun silk fibroin scaffolds for vascular cell growth. *Biomaterials* 2008; 29(14): 2217–2227.
13. Hodgkinson T, Chen Y, Bayat A, et al. Rheology and electrospinning of regenerated *Bombyx mori* silk fibroin aqueous solutions. *Biomacromolecules* 2014; 15(4): 1288–1298.
14. Ohgo K, Zhao C, Kobayashi M, et al. Preparation of nonwoven nanofibers of *Bombyx mori* silk, *Samia cynthia ricini* silk and recombinant hybrid silk with electrospinning method. *Polymer* 2003; 44(3): 841–846.
15. Sukigara S, Gandhi M, Ayutsede J, et al. Regeneration of *Bombyx mori* silk by electrospinning. Part 2: process optimization and empirical modeling using response surface methodology. *Polymer* 2004; 45(11): 3701–3708.
16. Min BM, Jeong L, Lee KY, et al. Regenerated silk fibroin nanofibers: water vapor-induced structural changes and their effects on the behavior of normal human cells. *Macromol Biosci* 2006; 6(4): 285–292.
17. Wang Y, Kim H-J, Vunjak-Novakovic G, et al. Stem cell-based tissue engineering with silk biomaterials. *Biomaterials* 2006; 27(36): 6064–6082.
18. Ayutsede J, Gandhi M, Sukigara S, et al. Regeneration of *Bombyx mori* silk by electrospinning. Part 3: characterization of electrospun nonwoven mat. *Polymer* 2005; 46(5): 1625–1634.
19. Jeong L, Lee KY, Liu JW, et al. Time-resolved structural investigation of regenerated silk fibroin nanofibers treated with solvent vapor. *Int J Biol Macromol* 2006; 38(2): 140–144.
20. Kang M, Jung R, Kim H-S, et al. Silver nanoparticles incorporated electrospun silk fibers. *J Nanosci Nanotechnol* 2007; 7(11): 3888–3891.
21. Zhu J, Shao H and Hu X. Morphology and structure of electrospun mats from regenerated silk fibroin aqueous solutions with adjusting pH. *Int J Biol Macromol* 2007; 41(4): 469–474.
22. Silva SS, Maniglio D, Motta A, et al. Genipin-modified silk-fibroin nanometric nets. *Macromol Biosci* 2008; 8(8): 766–774.
23. Wharram SE, Zhang X, Kaplan DL, et al. Electrospun silk material systems for wound healing. *Macromol Biosci* 2010; 10(3): 246–257.
24. Lee OJ, Ju HW, Kim JH, et al. Development of artificial dermis using 3D electrospun silk fibroin nanofiber matrix. *J Biomed Nanotechnol* 2014; 10(7): 1294–1303.
25. Jin H-J, Fridrikh SV, Rutledge GC, et al. Electrospinning *Bombyx mori* silk with poly(ethylene oxide). *Biomacromol* 2002; 3(6): 1233–1239.
26. Min B-M, Jeong L, Nam YS, et al. Formation of silk fibroin matrices with different texture and its cellular response to normal human keratinocytes. *Int J Biol Macromol* 2004; 34(5): 223–230.
27. McNamara LE, Burchmore R, Riehle MO, et al. The role of microtopography in cellular mechanotransduction. *Biomaterials* 2012; 33(10): 2835–2847.
28. Bacakova L, Filova E, Parizek M, et al. Modulation of cell adhesion, proliferation and differentiation on materials designed for body implants. *Biotechnol Advan* 2011; 29(6): 739–767.
29. Chen M, Patra PK, Warner SB, et al. Role of fiber diameter in adhesion and proliferation of NIH 3T3 fibroblast on electrospun polycaprolactone scaffolds. *Tissue Eng* 2007; 13(3): 579–587.
30. Kumbar SG, Nukavarapu SP, James R, et al. Electrospun poly(lactic acid-co-glycolic acid) scaffolds for skin tissue engineering. *Biomaterials* 2008; 29(30): 4100–4107.
31. Christopherson GT, Song H and Mao H-Q. The influence of fiber diameter of electrospun substrates on neural stem cell differentiation and proliferation. *Biomaterials* 2009; 30(4): 556–564.
32. Rüder C, Sauter T, Kratz K, et al. Influence of fibre diameter and orientation of electrospun copolyetheresterurethanes on smooth muscle and endothelial cell behaviour. *Clin Hemorheol Microcirc* 2013; 55(4): 513–522.
33. Badami AS, Kreke MR, Thompson MS, et al. Effect of fiber diameter on spreading, proliferation, and differentiation of osteoblastic cells on electrospun poly(lactic acid) substrates. *Biomaterials* 2006; 27(4): 596–606.
34. Bondar B, Fuchs S, Motta A, et al. Functionality of endothelial cells on silk fibroin nets: comparative study of micro-and nanometric fibre size. *Biomaterials* 2008; 29(5): 561–572.
35. Kilsdonk JW, Bogaard EH, Jansen PA, et al. An in vitro wound healing model for evaluation of dermal substitutes. *Wound Repair Regen* 2013; 21(6): 890–896.
36. Li Z, Yuan X-F, Haward SJ, et al. Non-linear dynamics of semi-dilute polydisperse polymer solutions in microfluidics: a study of a benchmark flow problem. *J Non-Newton Fluid* 2011; 166(16): 951–963.
37. Syed F, Ahmadi E, Iqbal SA, et al. Fibroblasts from the growing margin of keloid scars produce higher levels of collagen I and III compared with intralesional and extralesional sites: clinical implications for lesional site-directed therapy. *Br J Dermatol* 164(1): 83–96.
38. Hu Y, Zhang Q, You R, et al. The relationship between secondary structure and biodegradation behavior of silk fibroin scaffolds. *Adv Mater Sci Eng* 2012; 2012: 185905(5 pp).
39. Cao Y and Wang B. Biodegradation of silk biomaterials. *Int J Mol Sci* 2009; 10(4): 1514–1524.
40. Suarez E, Syed F, Alonso-Rasgado T, et al. Up-regulation of tension-related proteins in keloids: knockdown of Hsp27, α2β1-integrin, and PAI-2 shows convincing reduction of extracellular matrix production. *Plast Reconstr Surg* 2013; 131(2): 158e–173e.
41. Suarez E, Syed F, Rasgado TA, et al. Skin equivalent tensional force alters keloid fibroblast behaviour and phenotype. *Wound Repair Regen*. Epub ahead of print 21 July 2014. DOI: 10.1111/wrr.12215.
42. Koláčná L, Bakešová J, Varga F, et al. Biochemical and biophysical aspects of collagen nanostructure in the extracellular matrix. *Physiol Res* 2007; 56(Suppl. 1): 51–60.

43. Ichihara S, Inada Y and Nakamura T. Artificial nerve tubes and their application for repair of peripheral nerve injury: an update of current concepts. *Injury* 2008; 39: 29–39.
44. Yannas IV, Zhang M and Spilker MH. Standardized criterion to analyze and directly compare various materials and models for peripheral nerve regeneration. *J Biomater Sci Polym* 2007; 18(8): 943–966.
45. Toh Y-C, Ng S, Khong YM, et al. Cellular responses to a nanofibrous environment. *Nano Today* 2006; 1(3): 34–43.
46. Pham QP, Sharma U and Mikos AG. Electrospinning of polymeric nanofibers for tissue engineering applications: a review. *Tissue Eng* 2006; 12(5): 1197–1211.
47. Zhang LQ, Laato M, Muona P, et al. Normal and hypertrophic scars: quantification and localization of messenger RNAs for type I, III and VI collagens. *Br J Dermatol* 1994; 130(4): 453–459.
48. Spear SL, Sher SR, Al-Attar A, et al. Applications of acellular dermal matrix in revision breast reconstruction surgery. *Plast Reconstr Surg* 2014; 133(1): 1–10.
49. Dumanian GA. Discussion: applications of acellular dermal matrix in revision breast reconstruction surgery. *Plast Reconstr Surg* 2014; 133(1): 11–13.
50. Salzberg CA, Dunavant C and Nocera N. Immediate breast reconstruction using porcine acellular dermal matrix (Strattice™): long-term outcomes and complications. *J Plast Reconstr Aesthet Surg* 2013; 66(3): 323–328.
51. Mortarino E. Silk medical device for use in breast augmentation and breast reconstruction. Google patents WO2013082093 A, 2013.